SEMARAK ILMU PUBLISHING

Journal of XX

Journal homepage:
https://semarakilmu.com.my/journals/
ISSN: XXXX-XXXX

Impact Of Heat Source/Sink Towards MHD Stagnation Flow and Heat Transfer of GO-TiO_2-Ag/Water Nanofluid Over a Shrinking Surface

Nor Ain Azeany Mohd Nasir[1,2,*], Nooraini Zainuddin[3], Norihan Md Arifin[2,4], Nur Syahirah Wahid[4] and Ioan Pop[5]

[1] Department of Mathematics, Centre for Defence Foundation Studies, Universiti Pertahanan Nasional Malaysia, Kem Sungai Besi 57000 Kuala Lumpur, Malaysia.
[2] Institute for Mathematical Research, Universiti Putra Malaysia, 43400 UPM Serdang, Selangor, Malaysia.
[3] Department of Fundamental and Applied Sciences, Faculty of Science and Information Technology, Universiti Teknologi PETRONAS, 32610 Seri Iskandar, Perak, Malaysia.
[4] Department of Mathematics and Statistics, Faculty of Science, Universiti Putra Malaysia, 43400 UPM Serdang, Selangor, Malaysia.
[5] Department of Mathematics, Babes-Bolyai University, 400084 Cluj-Napoca, Romania.

ARTICLE INFO

Article history:
Received 29 October XXXX
Received in revised form 1 December XXXX
Accepted 9 December XXXX
Available online 10 December XXXX

Keywords:

Ternary hybrid nanofluid; shrinking surface; heat source/sink; MHD

ABSTRACT

This investigation aims to solve the mathematical modelling of magnetohydrodynamic (MHD) stagnation flow and heat transfer of GO-TiO_2-Ag/water nanofluid towards a shrinking surface problem. The model contains the impacts of suction/injection, radiation, magnetic field intensity, and heat source/sink parameters. By converting the governing equations into ordinary differential equations with applying similarity conversion and employing the bvp4c built-in solver in MATLAB software, numerical results are attained. Furthermore, the existence of GO as the ternary particles improves more the temperature profile but declining the velocity profile. This investigation promotes substantial understandings into heat transference achievement in MHD stagnation flow towards a shrinking surface, specifically with the interaction of GO particles and heat source/sink influences.

1. Introduction

Magnetohydrodynamic (MHD) stagnation flow is an essential domain of research in fluid dynamics, specifically when studying heat transfer anomaly. This flow system happens at the point where a fluid obtrudes on a solid plane, initiating a stagnation point. Nevertheless, when a magnetic field is directed to it, it causes electrical conductivity in the fluid, indicating complex connections between the fluid, magnetic field, and solid surface at the stagnation point. Recognizing MHD stagnation flow is vital because of its significance in countless engineering utilizations, such as in aerospace engineering and material processing. For aerospace engineering, the MHD influences on stagnation flow are critical for planning re-entry vehicles and administering heat transferal through atmospheric entry. Managing heat transferal at stagnation points can change product quality and effectiveness in materials processing, such as crystal development or metal modeling. Due to its significance in abundant domains, countless researchers have administered investigation on MHD. For precedent, Idris et al. [1] discovered that enhancing the MHD parameter driven to a heat transferal ratio improvement of above 9%, whereas Rafique et al. [2] declared an identical result, nevertheless, they also observed a reduce in the viscosity of the hybrid nanofluid. It is also important

to concentrate on the details administered by Mumtaz et al. [3], which declares that skin friction is enhanced concurrently with the MHD impact, and the influence is superior when utilizing a ternary hybrid nanofluid. Mahmood *et al.* [4] added to the literature that with the bits of help of MHD, the skin friction and heat transfer rate amplified together the volume fraction nanoparticles for the case using Al_2O_3-Cu-TiO_2/H_2O only. Furthermore, the flow of the fluid can be improved by adding more effects to the system, such as slip and suction factors, as demonstrated by Hussain *et al.* [5]. Several other factors have been proposed to improve further the heat transfer rate, for instance, thermal stratification with mixed convection by Jamrus *et al.* [6], hall current overheated rotating geometry by Ayub *et al.* [7] and heat generation, viscous dissipation, and joule heating effects by Rafique *et al.* [8].

The importance of radiation effects in optimising ternary hybrid nanofluid flow and heat transfer lies in several key aspects. The radiation plays a significant role in the heat transfer process, especially in situations where conventional conduction and convection mechanisms may be limited. The inclusion of radiation effects can lead to improved thermal performance and enhanced heat transfer rates in nanofluid-based systems. This claim was proven when Wahid et al. [9] reported that their investigation results highlighted the effectiveness of increasing the boundary suction parameter and reducing thermal radiation to enhance heat transfer within the specific conditions of a ternary hybrid nanofluid. In real-life applications, the significance of radiation effects in fluid flow and heat transfer is evident across various sectors. For example, in solar thermal systems where nanofluids are used as heat transfer fluids, radiation effects can significantly impact system efficiency and energy capture. This phenomenon can lead to more efficient solar collectors and thermal energy storage systems. Additionally, in industries such as aerospace and automotive engineering, where thermal management is crucial for component performance and reliability, radiation effects play a vital role. It is noted that radiation can lead to improved cooling performance, reduced energy consumption, and enhanced system durability in high-temperature environments. As Maranna et al. [10] suggested, using second-grade fluid as the ternary hybrid nanofluid will theoretically improve the thermal layer with high-temperature profiles. A similar finding has been reported by Mahabaleshwar *et al.* [11], with added to the report results revealing that the heat transfer performance of the ternary nanofluid phase is better than that of the dusty phase. Furthermore, in medical applications such as hyperthermia treatment, where precise control of temperature distribution is critical, radiation effects can be utilised to optimise heat transfer within nanofluid-based systems, leading to more effective therapeutic outcomes. Sharma *et al.* [12] proposed that their discovery provides advantages for clinical researchers, as their study observed an increase in entropy generation and the Bejan number with the enhancement of the Brinkman and radiation parameters. Numerous researchers have investigated the impact of radiation towards ternary hybrid nanofluid flows in various circumstances, resulting in diverse findings. For instance, Aich *et al.* [13] investigated the heat capacity for Al_2O_3-CuO-Cu/water, while Khan *et al.* [14] considered the ternary hybrid Casson fluid over a nonlinear stretching disk.

Understanding and improving the effect of heat absorption/generation can result in improved heat management and enhanced performance in various engineering applications. Mahmood *et al.* [15] proposed that investigating heat absorption/ generation can provide scientists and engineers with a starting point for optimising the relevant parameters to achieve optimal outcomes in practical applications. In real-life applications, the significance of heat generation/absorption effects in fluid flow and heat transfer is evident across diverse industries. For instance, in the field of energy generation, optimising heat generation/absorption effects can improve the efficiency of thermal power plants and enhance energy conversion processes. It is important to know which effects can amplify the heat transfer rate. For example, Sajid et al. [16] suggested that heat generation and

absorption with the help of the radiation effect can augment the heat transfer rate. Moreover, in industries such as materials processing and manufacturing, where precise control of temperature and heat transfer is critical for product quality and efficiency, optimising heat generation/absorption effects can lead to advancements in product development, process optimisation, and overall productivity. Several parameters have been found that can control heat transfer together with heat absorption/generation, such as Casson fluid, thermal conductivity of the fluid, diffusion coefficient and wedge parameter, as reported by Sajid et al. [17]. Furthermore, in medical applications such as biomedical engineering, understanding, and controlling heat generation/absorption effects are crucial for medical device design. In ordinance with this application, Alqahtani et al. [18] have investigated energy transportation using Carreau Yasuda fluid. The results stated that the magnetic dipole plays a significant role together with the heat absorption/generation in increasing the thermal energy transmission of trihybrid nanofluid and reducing the velocity profile. Then, the investigation was further improved with the Fourier heat flux model over a disk by Alqawasmi *et al.* [19], who observed that reducing the magnetic parameter decreases fluid velocity but increases fluid temperature over a spinning disc, with notable effects on temperature distribution and heat absorption/generation, particularly significant for ternary composite nanofluid. The latest finding by Mishra *et al.* [20], demonstrated that the heat transfer rate is the highest for the cone surface rather than the flat surface when heat absorption/generation acts on the surface.

Based on the above-mentioned literature, this study intends to assess the ternary hybrid nanofluid flow and heat transfer of magnetohydrodynamic (MHD) at the stagnation point on a shrinking sheet. The impacts acting on the system involved in this study are assumed to be radiation and heat absorption/generation factors. The governing equations derived based on the problem mentioned above are then reduced to higher-order ordinary differential equations (ODEs) coupled with a boundary value problem. The ODEs are then solved using the famous solver called bvp4c, which is built into MATLAB software. The stability of the solutions has been shown by Wahid *et al.* [21]. Hence, the results for the second solution will not be discussed but will still be reported since the flow might be useful in future and to avoid the misconstruction of the flow and heat transfer characteristics [22].

2. Methodology

A steady two-dimensional MHD stagnation-point flow of a ternary hybrid nanofluid towards the shrinkage surface is shown in Figure 1. In the Cartesian coordinate system, the x and y axes represent dimensions where the x-axis runs parallel to the surface, and the y-axis extends in a direction that is perpendicular to the surface. The initiation of the flow occurs at $y \geq 0$. It is assumed that the velocity of the inviscid flow is $u_e(x)$, while the velocity of the retracting sheet is $u_w(x)$. It is also notable that $v = v_0$ is the mass flux where v_0 is known as injection parameter (positive), suction parameter (negative) and permeable (equals to zero). Considering the surface-normal direction of the transverse magnetic field is denoted by B_0, the temperature of the free stream is represented by T_∞, and the temperature of the sheet is denoted as T_w.

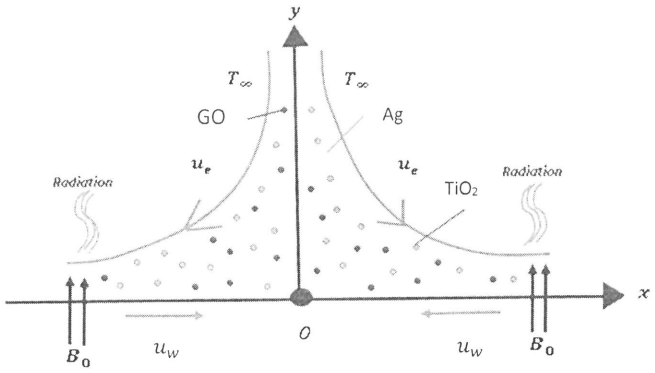

Fig. 1 Physical model for shrinking surface.

The governing equations that dictate the assumptions regarding flow, as previously mentioned, can be outlined as follows, according to Wahid *et al.* [21].

$$\frac{\partial u}{\partial x}+\frac{\partial v}{\partial y}=0, \tag{1}$$

$$u\frac{\partial u}{\partial x}+v\frac{\partial u}{\partial y}=u_e\frac{du_e}{dx}+\frac{\mu_{thnf}}{\rho_{thnf}}\left(\frac{\partial^2 u}{\partial y^2}\right)-\frac{\sigma_{thnf}{B_0}^2}{\rho_{thnf}}(u-u_e), \tag{2}$$

$$u\frac{\partial T}{\partial x}+v\frac{\partial T}{\partial y}=\frac{k_{hnf}}{(\rho C_p)_{hnf}}\left(\frac{\partial^2 T}{\partial y^2}\right)+\frac{\mu_{hnf}}{(\rho C_p)_{hnf}}\left(\frac{\partial u}{\partial y}\right)^2-\frac{1}{(\rho C_p)_{hnf}}\frac{\partial q_r}{\partial y}+\frac{Q\square}{(\rho C_p)_{thnf}}(T-T_\infty), \tag{3}$$

An adequate boundary condition, when combined,

$$u=u_w(x)=bx,\quad v=v_0,\quad T=T_w \quad \text{at } y=0,$$

$$u\to u_e(x)=ax,\quad T\to T_\infty \quad \text{as } y\to\infty. \tag{4}$$

The text outlines that the symbols $\mu,\rho,\sigma,\rho C_p,k$ represent dynamic viscosity, density, electrical conductivity, heat capacity, and thermal conductivity, correspondingly. The notation $thnf$ is used to denote ternary hybrid nanofluid, with ϕ_1, ϕ_2 and ϕ_3 indicating the volume percentages of graphene oxide (GO), titanium dioxide (TiO_2), and silver (Ag) nanoparticles, respectively. Water (H_2O) is utilised as the base fluid. Table 1 presents a detailed examination of the relationship between the thermophysical properties and the composition of ternary hybrid nanofluids.

Table 1
The correlation between the thermophysical properties of ternary hybrid nanofluids and the shape factors of their nanoparticles. (Ref. Mumtaz *et al.* [3])

Properties	Ternary Hybrid nanofluid
Density	$\frac{\rho_{thnf}}{\rho_f}=(1-\phi_3)\left[(1-\phi_2)\left\{(1-\phi_1)+\phi_1\frac{\rho_{s1}}{\rho_f}\right\}+\phi_2\frac{\rho_{s2}}{\rho_f}\right]+\phi_3\frac{\rho_{s3}}{\rho_f}$
Dynamic viscosity	$\frac{\mu_{thnf}}{\mu_f}=\frac{1}{(1-\phi_1)^{2.5}(1-\phi_2)^{2.5}(1-\phi_3)^{2.5}}$

Electrical Conductivity	$\frac{\sigma_{thnf}}{\sigma_f} = \left[\frac{(1+2\phi_2)\sigma_{s3}+(1-2\phi_3)\sigma_{hnf}}{(1-\phi_2)\sigma_{s3}+(1-\phi_3)\sigma_{hnf}}\right]\frac{\sigma_{hnf}}{\sigma_f}$ where $\frac{\sigma_{hnf}}{\sigma_{nf}} = \frac{\sigma_{s2}+2\sigma_{nf}-2\phi_2(\sigma_{nf}-\sigma_{s2})}{\sigma_{s2}+2\sigma_{nf}+\phi_2(\sigma_{nf}-\sigma_{s2})}$ and $\frac{\sigma_{nf}}{\sigma_f} = \frac{\sigma_{s1}+2\sigma_f-2\phi_1(\sigma_f-\sigma_{s1})}{\sigma_{s1}+2\sigma_f+\phi_1(\sigma_f-\sigma_{s1})}$
Heat capacity	$\frac{(\rho C_p)_{thnf}}{(\rho C_p)_f} = (1-\phi_3)\left[(1-\phi_2)\left\{(1-\phi_1)+\phi_1\frac{(\rho C_p)_{s1}}{(\rho C_p)_f}\right\}+\phi_2\frac{(\rho C_p)_{s2}}{(\rho C_p)_f}\right]+\phi_3\frac{(\rho C_p)_{s3}}{(\rho C_p)_f}$
Thermal conductivity	$\frac{k_{thnf}}{k_f} = \left[\frac{k_{s3}+2k_{hnf}-2(k_{hnf}-k_{s3})\phi_3}{k_{s3}+2k_{hnf}+(k_{hnf}-k_{s3})\phi_3}\right]\left(\frac{k_{hnf}}{k_f}\right)$ where $\frac{k_{hnf}}{k_{nf}} = \frac{k_{s2}+(m-1)k_{nf}-(m-1)(k_{nf}-k_{s2})\phi_2}{k_{s2}+(m-1)k_{nf}+(k_{nf}-k_{s2})\phi_2}$ and $\frac{k_{nf}}{k_f} = \frac{k_{s1}+(m-1)k_f-(m-1)(k_f-k_{s1})\phi_1}{k_{s1}+(m-1)k_f+(k_f-k_{s1})\phi_1}$

Table 2 presents the data for computing the thermophysical characteristics of the hybrid nanofluid, as listed in Table 1.

Table 2
Thermophysical properties values of GO, TiO_2, Ag, and H_2O. (Ref. Redouane *et al.* [23])

Thermophysical Properties	GO	TiO_2	Ag	H_2O
Dynamic viscosity $\mu\ (kgm^{-1}s^{-1})$	-	-	-	0.000855
Density $\rho\ (kgm^{-2})$	1800	4250	10500	997.1
Electrical Conductivity $\sigma\ (Sm^{-1})$	6.3×10^7	2.6×10^6	6.3×10^7	5.5×10^{-6}
Specific Heat capacity $C_p\ (Jkg^{-1}K^{-1})$	717	686	235	4179
Thermal conductivity $k\ (Wm^{-1}K^{-1})$	5000	8.9538	429	0.613

To simplify the complexity of solving the mathematical modelling Eqs. (1) – (4), they must be condensed into ordinary differential equations (ODEs). This can be efficiently done through the employment of similarity transformation, which involves the use of a suitable similarity variable, as detailed by Wahid *et al.* [21].

$$\psi = \sqrt{av_f}xf(\eta), \quad \theta(\eta) = \frac{T-T_m}{T_m-T_\infty}, \quad \eta = \sqrt{\frac{a}{v_f}}y. \tag{5}$$

The stream function is associated with velocity components as given,

$$u = axf'^{(\eta)}, \quad v = -\sqrt{av_f}f(\eta). \tag{6}$$

By differentiating and substituting Eqs. (5) and (6) into Eqs. (1) through (4), new equations can be derived.

$$\frac{\phi_3}{\phi_4}f'''-f'^2+ff''-\frac{\phi_5}{\phi_4}M(f'-1)+1=0, \tag{7}$$

$$\frac{1}{\phi_2 Pr}[\phi_1 + Rd]\vartheta'' + \frac{\phi_3}{\phi_2} Ec\, f''^2 + \frac{\xi}{\phi_2}\vartheta + f\,\vartheta' = 0, \tag{8}$$

along with an appropriate boundary condition,

$$f' = \alpha, \quad f = S, \quad \vartheta = 1 \ \ at\ y = 0, \tag{9}$$

$$f' \to 1, \quad \vartheta \to 0 \ \ as\ y \to \infty .$$

In Eqs. (7) to (9), the parameter is defined as per Table 3.

Table 3
List of parameters associated with Eqs. (7)–(9).

Parameter	Equation
Magnetic parameter, M	$M = \frac{\sigma_f {B_0}^2}{a\rho_f}$
Ternary hybrid nanofluid parameter	$\phi_1 = \frac{k_{thnf}}{k_f}$, $\phi_2 = \frac{(\rho C_p)_{thnf}}{(\rho C_p)_f}$, $\phi_3 = \frac{\mu_{thnf}}{\mu_f}$, $\phi_4 = \frac{\rho_f}{\rho_{thnf}}$, $\phi_5 = \frac{\sigma_{thnf}}{\sigma_f}$
Radiation parameter, Rd	$Rd = \frac{16\sigma^* {T^3}_\infty}{3k^* k_f}$
Eckert number, Ec	$Ec = \frac{a{u_w}^2}{(T_w - T_\infty)(C_p)_f}$
Heat source/sink, ξ	$\xi = \frac{Qa}{(\rho C_p)_f}$
Suction/injection parameter, S	$S = \frac{v_0}{-\sqrt{av_f}}$
Stretching/shrinking parameter, α	$\alpha = \frac{b}{a}$

The physical quantities essential to Eqs. (7)–(9) are recognised as skin friction and the Nusselt number.

$$\text{Skin friction } C_f = \frac{\mu_{thnf}}{\rho_f {u_e}^2}\left(\frac{\partial u}{\partial y}\right)_{y=0}, \tag{10}$$

$$\text{local Nusselt number } Nu_x = -\frac{x k_{thnf}}{k_f (T_w - T_\infty)}\left(\frac{\partial T}{\partial y}\right)_{y=0}.$$

Arranging the Eq. (10) and substituting Eq. (5) give out,

$$Re^{1/2}{}_x\, C_f = \phi_3 f''(0) \ \text{ and } \ Re_x{}^{-1/2}\, Nu_x = -\phi_1 \theta'(0), \tag{11}$$

where $Re_x = u/v_f$ is Reynold's number.

3. Results

Using the bvp4c solver within MATLAB software, the system of equations, including the Eqs. (7)-(8), along with the specified boundary conditions Eq. (9), is solved numerically. The numerical results are presented through tables and figures. Precisely, Table 4 displays the relative values of the reduced skin friction coefficient for several values of parameters when $\phi_3 = \phi_4 = 1, M = S = 0$. These results indicate a significant agreement between the current findings and previous studies conducted by Aminuddin *et al.* [24] and Nasir *et al.* [25]. The established numerical approach demonstrates confidence in solving the current problem. Notably, the nanoparticle concentration and heat source/sink parameters considered in this study are within the ranges $0 \leq \varphi_3 \leq 0.03$ and $-0.03 \leq \xi \leq 0.03$, with the magnetic parameter $0.01 \leq M \leq 0.07$, the radiation parameter $0.0 \leq Rd \leq 1.5$ and an Eckert number of $0.1 \leq Ec \leq 0.3$.

Table 4
Numerical solution for skin friction when $\varphi_1 = \varphi_2 = \varphi_3 = 0,\ M = \xi = S = 0,\ Rd = 0,\ Ec = 0,\ \alpha = 0$ and $Pr = 6.2$ (water).

α	Aminuddin et al. [24]		Nasir et al. [25]		Current solution	
	Upper solution	Lower solution	Upper solution	Lower solution	Upper solution	Lower solution
-0.25	402240775	-	1.40224078	-	1.402240807	-
-0.5	1.495669733	-			1.495669765	-
-0.75	1.489298201	-	1.48929820	-	1.489298236	-
-1.0	1.328816835	0.000000000	1.32881685	0.0	1.328816875	0.0
-1.1	1.186680243	0.049228914	1.1866805	0.049229	1.186680258	0.049228955
-1.15	1.082231127	1.8223113	0.11670214	0.1167022	1.082231136	0.116701735
-1.2	0.932473313	0.233649705	0.93247331	0.23364973	0.932473318	0.233647245
-1.2465	0.584281488	0.554296326	0.58428116	0.55429619	0.584281486	0.553572833
-1.24657					0.574525287	0.562136224

Table 5
Numerical results for skin friction coefficient and Nusselt number for various values of several parameters when $\alpha = -2.5, S = 2.0, \varphi_1 = 0.01, \varphi_2 = \varphi_3 = 0.02, \xi = 0.1$(heat source) and $Pr = 6.2$ where [] indicate lower solution.

M	Rd	Ec	C_f	Nu_x
0.01	0.5	0.1	6.593368585, [0.843041148]	0.428775204, [-20.974511337]
0.04			6.507550744, [0.908656715]	0.465482092, [-15.561502660]
0.07			6.419172005, [0.977360124]	0.502646827, [-11.884957299]
0.04	0.0		6.507550739,	0.852023272,

			[0.908656712]	[-44.506121539]
	0.5		6.507550744, [0.908656715]	0.465482092, [-15.561502660]
	1.0		6.507550744, [0.908656724]	0.303238002, [-7.064164377]
	1.5		6.507550740, [0.908656729]	0.227372169, [-3.880797949]
	1.0	0.1	6.507550744, [0.908656724]	0.303238002, [-7.064164377]
		0.2	6.507550754, [0.908656715]	-4.665105047, [-16.619604371]
		0.3	6.507550756, [0.908656714]	-9.633448097, [-26.175044376]

3.1 Skin friction coefficient and Nusselt number

Based on the numerical results illustrated in Table 5, it is evident that the magnetic parameter M have significantly affected skin friction. It is due to the Lorentz force induced by M which can significantly alter the flow patterns with the bits of help of the particles of ternary hybrid nanofluid. The impact is further amplified when the system has heat source parameters. For this problem, the heat source uniforms the heating process, smoothing the flow and resulting in reduced skin friction. It is noted that the suction parameter tends to pull the fluid towards the surface by altering the boundary layer thickness and the fluid flow velocity. This phenomenon leads to the augmentation of the Nusselt number. The radiation parameter further influences the heat transport ratio of the fluid flow. The radiation parameter contributes to the changes in temperature profile and heat dissipation, while the Eckert number would lead to variations in flow patterns and temperature differences, which would further affect the heat transportation ratio, hence reducing the skin friction on the shrinking surface.

However, it is well known that radiation can influence thermal energy transportation in fluid flow. It is eye-catching that the radiation parameter can further reduce the heat transportation ratio, as shown in Table 5. When the surface is shrinking, a higher radiation parameter leads to a decline in the Nusselt number. The reason for this is that higher radiation levels with the combination of magnetic, Eckert number and suction parameters result in more heat dispersion from the surface, decreasing the total heat transport rate to the fluid. As the Eckert number ascends, it indicates a greater dominance of thermal energy over kinetic energy in the fluid. An augmentation in the Eckert number coupled with an elevated magnetic parameter might result in diminished Nusselt numbers on a shrinking surface. The reason for this is that the combined influence of magnetic forces and increased thermal energy can facilitate the dispersion of heat away from the surface, resulting in a decrease in the Nusselt number.

Table 6
Numerical results for skin friction coefficient and Nusselt number for various values of several parameters when $\alpha = -2.5, S = 2.0, \varphi_1 = 0.01, \varphi_2 = 0.02, \xi = -0.02$(heat sink) and $Pr = 6.2$.

M	Rd	Ec	C_f	Nu_x
0.01	0.5	0.1	6.593368584,	0.716346134,

			[0.843041159]	[-5.099046470]
0.03			6.536430282, [0.886452280]	0.742443718, [-4.504436552]
0.04			6.507550743, [0.908656742]	0.755594197, [-4.225334938]
0.03	0.0		6.536430277, [0.886452263]	1.206993868, [-10.181230553]
	0.5		6.536430282, [0.886452280]	0.742443718, [-4.504436552]
	1.0		6.536430278, [0.886452284]	0.534840168, [-2.282368163]
	1.5		6.536430278, [0.886452267]	0.428337686, [-1.282948244]
	1.0	0.1	6.536430278, [0.886452284]	0.534840168, [-2.282368163]
		0.2	6.536430291, [0.886452270]	-4.312986643, [-8.161284740]
		0.3	6.536430294, [0.886452262]	-9.160813453, [-14.040201295]

According to the numerical data shown in Table 6, the presence of a magnetic field can result in a decrease in skin friction in the context of heat sinking. The Lorentz force can oppose the frictional forces present in the fluid, leading to a more streamlined flow over the contracting surface. In addition, the inclusion of a heat sink can also influence skin friction, hence enhancing the complexity of the situation. Combining heat sinking with suction makes it possible to further decrease skin friction by improving the stability of flow and minimising disruptions in the flow. It is important to note that heat sinking causes a reduction in thermal energy in the fluid, leading to a decrease in Nusselt number. Furthermore, with the presence of a heat sink, the radiation parameter enhances the reduction of the heat transportation ratio due to less thermal energy being available in the boundary layer. It is also worth mentioning that when heat is taken from the fluid (heat sinking), the thermal energy component reduces compared to kinetic energy. A more significant Eckert number, paired with heat sinking, can contribute to lower skin friction. This is because the reduced thermal energy component results in less energy available for heat dissipation and frictional losses, resulting in a lower heat transportation ratio. It is eye-catching that the magnetic parameter augmented the skin friction while diminishing the heat transportation ratio. This phenomenon occurs due to the reduction of viscous dissipation, which helps maintain higher kinetic energy in the flow, lowering skin friction and enhancing the heat transportation ratio along the surface.

3.2 Velocity and temperature profiles

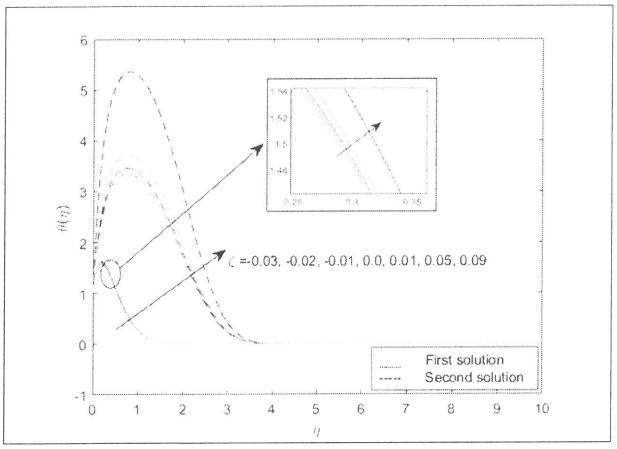

Fig. 2 Distribution of temperature profile for several values of heat source and sink when $M = 0.03$, $Ec = 0.3$, $S = 2.0, Pr = 6.2, Rd = 1.0$ and ternary hybrid nanofluid parameters $\phi_1 = 0.01$, $\phi_2 = 0.02, \phi_3 = 0.02$.

The temperature profile of a fluid system is impacted by several elements, including heat source and heat sink properties as depicted in Figure 2. When the heat source parameter rises, it brings extra thermal energy into the fluid system. The heat source parameter represents a source of heat production inside the fluid. This produced heat adds to raise the temperature of the fluid, especially in the proximity of the heat source. The heat sink parameter, on the other hand, represents a mechanism for heat absorption or dissipation from the fluid system. A reduction in the heat sink parameter signifies lower heat absorption or dissipation, enabling more thermal energy to remain within the fluid. With a lower heat sink value, there is less ability for the fluid to absorb or disperse heat. This lower cooling action results in greater temperatures inside the fluid.

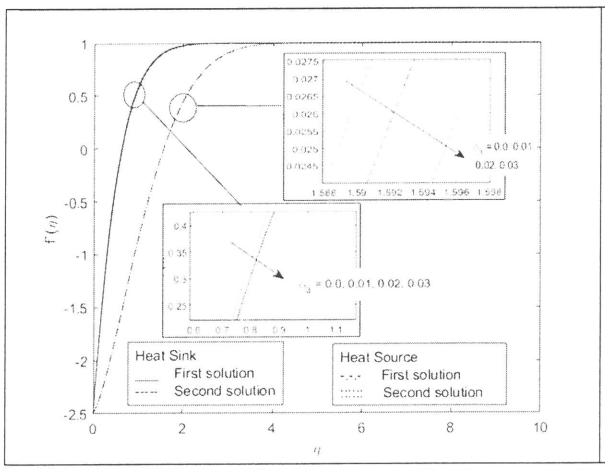

Fig. 3 Distribution of velocity profile for several values of GO concentration values when heat source ($\xi = 0.1$), heat sink ($\xi = -0.03$), $M = 0.03$, $Ec = 0.3$, $S = 2.0, Pr = 6.2, Rd = 1.0$ and hybrid nanofluid parameters $\phi_1 = 0.01, \phi_2 = 0.02$.

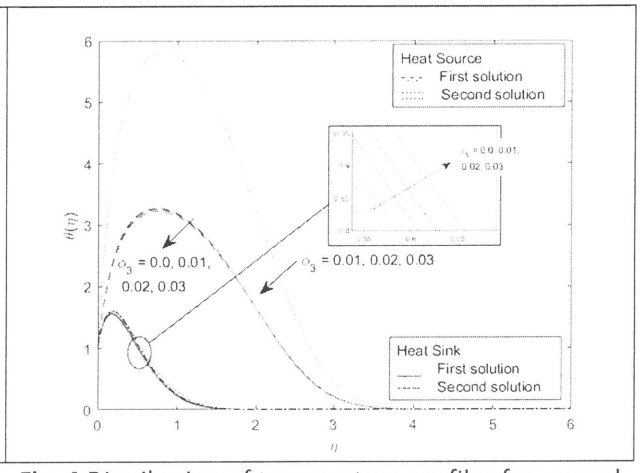

Fig. 4 Distribution of temperature profiles for several values of GO concentration when heat source ($\xi = 0.1$), heat sink ($\xi = -0.03$), $M = 0.03, Ec = 0.3$, $S = 2.0, Pr = 6.2, Rd = 1.0$ and hybrid nanofluid parameters $\phi_1 = 0.01, \phi_2 = 0.02$.

The increase in concentration of GO particles in a fluid flow can alter the fluid's velocity, especially when considering the influences of heat source and heat sink factors, as illustrated in Figure 3. GO

particles, especially at larger quantities, can enhance the viscosity of the fluid. This is because GO particles prefer to interact with the fluid molecules, producing an impediment to their flow. Furthermore, more significant concentrations of GO particles can lead to improved thermal conductivity and heat transfer within the fluid in the presence of a heat source. This can result in localised temperature changes and convective currents, which may modify flow patterns and diminish overall fluid velocity. Conversely, a heat sink characteristic describes a method for heat dissipation or absorption from the fluid. A reduction in the heat sink value means less heat dissipation, leading to greater temperatures in the fluid. Higher temperatures might promote thermal expansion of the fluid, which, along with increased viscosity owing to GO particles, further inhibits fluid flow and lowers velocity.

The increase in the concentration of GO particles in a fluid flow can cause the temperature profile of the fluid to rise, as pictured in Fig. 4. This is especially true when taking into account the characteristics of the heat source and heat sink. As the quantity of graphene oxide (GO) particles in the fluid rises, the thermal conductivity of the fluid likewise increases. Consequently, the fluid enables more effective heat transmission, resulting in elevated temperatures in areas affected by the heat source. Increased concentrations of graphene oxide (GO) particles improve thermal conduction, enabling the fluid to carry heat away from the heat source area more efficiently. This can lead to a more even dispersion of thermal energy over the fluid, resulting in an overall elevation of the temperature profile. Conversely, a higher concentration of GO particles can significantly improve thermal conductivity, making it easier for heat to move away from locations with lower temperatures, such as heat sink zones. This can diminish the efficiency of heat dissipation and contribute to elevated temperatures in the fluid.

4. Conclusions

This research has examined MHD stagnation point flow and heat transfer characteristics of a ternary hybrid nanofluid across a shrinking plate, with a specific emphasis on the influence of radiation and heat generation/absorption. The approach employed in this study entailed the reduction of the governing partial differential equations to ordinary differential equations by the utilisation of similarity transformations. Subsequently, the numerical solution of these ordinary differential equations was obtained utilising the bvp4c built-in solver inside the MATLAB program. Hence, the results have yielded significant insights into the impact of several parameters on the features of flow and heat transfer as follows:

- The net impact is a rise in the temperature profile throughout the fluid system, particularly in locations influenced by the heat source and where heat dissipation is constrained due to lower heat sink capacity.
- The escalation in GO particle concentration in a fluid flow, especially under the impact of heat source and heat sink parameters, leads to increased viscosity, thermal effects, and particle interactions, all of which collectively contribute to a reduction in fluid flow velocity.
- The interaction of heat source and heat sink parameters, along with an increased concentration of GO particles, leads to a collective impact on the fluid flow. This results in several combined effects, including improved thermal conductivity, decreased heat dissipation, enhanced convection, and frictional heating. As a result, the temperature profile of the fluid experiences an overall increase.

This research can be expanded by considering non-Newtonian ternary hybrid nanofluids, given their extensive applications in various industries. It is advisable to extend the study to optimize the

mathematical model and analyse the entropy generation, providing valuable insights into the utilization and efficiency of the model.

Acknowledgement

The researchers express their gratitude to the Ministry of Higher Education Malaysia, University Putra Malaysia, and National Defence University of Malaysia for their valuable supports in facilitating this study.

References

[1] Idris S, Jamaludin A, Nazar R and Pop I. Radiative MHD flow of hybrid nanofluid over permeable moving plate with Joule heating and thermal slip effects, *Alexandria Engineering Journal* 83 (2023): 222-233. https://doi.org/10.1016/j.aej.2023.09.065

[2] Rafique K, Mahmood Z and Khan U. Mathematical analysis of MHD hybrid nanofluid flow with variable viscosity and slip conditions over a stretching surface, *Materialstoday Communications* 36 (2023), 106692. https://doi.org/10.1016/j.mtcomm.2023.106692

[3] Mumtaz M, Islam S, Ullah H and Shah Z. Chemically reactive MHD convective flow and heat transfer performance of ternary hybrid nanofluid past a curved stretching sheet, *Journal of Molecular Liquids* 390(Part B) (2023), 123179. https://doi.org/10.1016/j.molliq.2023.123179

[4] Mahmood Z, Eldin SM, Rafique K and Khan U. Numerical analysis of MHD tri-hybrid nanofluid over a nonlinear stretching/shrinking sheet with heat generation/absorption and slip conditions, *Alexandria Engineering Journal* 76 (2023), 799-819. https://doi.org/10.1016/j.aej.2023.06.081

[5] Hussain Z, Aljuaydi F, Ayaz M and Islam S. Enhancing thermal efficiency in MHD kerosene oil-based ternary hybrid nanofluid flow over a stretching sheet with convective boundary conditions, *Results in Engineering* 22 (2024), 102151. https://doi.org/10.1016/j.rineng.2024.102151

[6] Jamrus FN, Waini I, Khan U and Ishak A. Effects of magnetohydrodynamics and velocity slip on mixed convective flow of thermally stratified ternary hybrid nanofluid over a stretching/shrinking sheet, *Case Studies in Thermal Engineering* 55 (2024), 104161. https://doi.org/10.1016/j.csite.2024.104161

[7] Ayub A, Asjad MI, Al-Malki MAS, Khan S, Eldin SM and El-Rahman MA. Scrutiny of nanoscale heat transport with ion-slip and hall current ternary MHD cross nanofluid over heated rotating geometry, *Case Studies in Thermal Engineering* 53 (2024), 103833. https://doi.org/10.1016/j.csite.2023.103833

[8] Rafique K, Mahmood Z, Adnan, Khan U, Muhammad T, Mir A, Aich W and Kolsi L. Unsteady MHD flow analysis of hybrid nanofluid over a shrinking surface with porous media and heat generation: Computational study on entropy generation and Bejan number, *International Journal of Heat and Fluid Flow* 107 (2024), 109419. https://doi.org/10.1016/j.ijheatfluidflow.2024.109419

[9] Wahid NS, Arifin NM, Yahaya RI, Khashi'ie NS and Pop I. Impact of suction and thermal radiation on unsteady ternary hybrid nanofluid flow over a biaxial shrinking sheet, *Alexandria Engineering Journal* 96 (2024), 132-141. https://doi.org/10.1016/j.aej.2024.03.079

[10] Maranna T, Mahabaleshwar US, Perez LM and Manca O. Flow of viscoelastic ternary nanofluid over a shrinking porous medium with heat Source/Sink and radiation, *Thermal Science and Engineering Progress* 40 (2023), 101791. https://doi.org/10.1016/j.tsep.2023.101791

[11] Mahabaleshwar US, Maranna T, Perez LM, Bognar GV and Oztop HF. An impact of radiation on laminar flow of dusty ternary nanofluid over porous stretching/shrinking sheet with mass transpiration, *Results in Engineering* 18 (2023), 101227. https://doi.org/10.1016/j.rineng.2023.101227

[12] Sharma BK, Sharma P, Mishra NK, Noeiaghdam S and Fernandez-Gamiz U. Bayesian regularization networks for micropolar ternary hybrid nanofluid flow of blood with homogeneous and heterogeneous reactions: Entropy generation optimization, *Alexandria Engineering Journal* 77 (2023), 127-148. https://doi.org/10.1016/j.aej.2023.06.080

[13] Aich W, Sarfraz G, Said NM, Bilal M, Elhag AFA and Hassan AM. Significance of radiated ternary nanofluid for thermal transport in stagnation point flow using thermal slip and dissipation function, *Case Studies in Thermal Engineering* 51 (2023), 103631. https://doi.org/10.1016/j.csite.2023.103631

[14] Khan D, Ali G, Kumam P, Sitthithakerngkiet K and Jarad F. Heat transfer analysis of unsteady MHD slip flow of ternary hybrid Casson fluid through nonlinear stretching disk embedded in a porous medium, *Ain Shams Engineering Journal* 15(2) (2024), 102419. https://doi.org/10.1016/j.asej.2023.102419

[15] Mahmood Z, Khan U, Rafique K and Eldin SM. Numerical analysis of ternary hybrid nanofluid flow over a stagnation region of stretching/shrinking curved surface with suction and Lorentz force, *Journal of Magnetism and Magnetic Materials* 573 (2023), 170654. https://doi.org/10.1016/j.jmmm.2023.170654

[16] Sajid T, Jamshed W, Eid MR, Algarni S, Alqahtani T, Ibrahim RW, Irshad K, Hussain SM and El-Din SM. Thermal case examination of inconstant heat source (sink) on viscous radiative Sutterby nanofluid flowing via a penetrable rotative cone, *Case Studies in Thermal Engineering* 48 (2023), 103102. https://doi.org/10.1016/j.csite.2023.103102

[17] Sajid T, Gari AA, Jamshed W, Eid MR, Islam N, Irshad K, Altamirano GC and El-Din SM. Case study of autocatalysis reactions on tetra hybrid binary nanofluid flow via Riga wedge: Biofuel thermal application, *Case Studies in Thermal Engineering* 47 (2023), 103058. https://doi.org/10.1016/j.csite.2023.103058

[18] Alqahtani AM, Bilal M, Elsebaee FAA, Eldin SM, Alsenani TR and Ali A. Energy transmission through Carreau Yasuda fluid influenced by ethylene glycol with activation energy and ternary hybrid nanocomposites by using a mathematical model, *Heliyon* 9(4) (2023), e14740. https://doi.org/10.1016/j.heliyon.2023.e14740

[19] Alqawasmi K, Alharbi KAM, Farooq U, Noreen S, Imran M, Akgul A, Kanan M and Asad J. Numerical approach toward ternary hybrid nanofluid flow with nonlinear heat source-sink and Fourier heat flux model passing through a disk, *International Journal of Thermofluids* 18 (2023), 100367. https://doi.org/10.1016/j.ijft.2023.100367

[20] Mishra A, Rawat SK, Yaseen M and Pant M. Development of machine learning algorithm for assessment of heat transfer of ternary hybrid nanofluid flow towards three different geometries: Case of artificial neural network, *Heliyon* 9(11) (2023), e21453. https://doi.org/10.1016/j.heliyon.2023.e21453

[21] Wahid NS., Arifin NM., Pop I., Bachok N., and Hafidzuddin MEH. MHD stagnation-point flow of nanofluid due to a shrinking sheet with melting, viscous dissipation and Joule heating effects, *Alexandria Engineering Journal*

[22] Khashi'ie, NS., Arifin, NM., Nazar, R., Hafidzuddin, EH., Wahi, N., and Pop, I. Mixed Convective Flow and Heat Transfer of a Dual Stratified Micropolar Fluid Induced by a Permeable stretching/Shrinking Sheet, *Entropy*, 21 (2019), 1162. https://doi.org/10.3390/e21121162

[23] Redouane F., Jamshed W., Devi SSU., Prakash M., Nasir NAAM, Hammouch Z., Eid MR, Nisar KS., Mohammed AB., Abdel-Aty A., Yahia IS., and Eed EM. Heat flow saturate of Ag/MgO-water hybrid nanofluid in heated trigonal enclosure with rotate cylindrical cavity by using Galerkin finite element, *Scientific Reports* 12 (2022) 2302. https://doi.org/10.1038/s41598-022-06134-6

[24] Aminuddin NA, Nasir NAAM, Jamshed W, Abdullah N, Ishak A, Pop I and Eid MR. Velocity and thermal slip impact towards GOMoS2/C3H8O3 hybridity nanofluid flowing via a moving riga plate, *Ain Shams Engineering Journal* 15 (2024), 102648. https://doi.org/10.1016/j.asej.2024.102648

[25] Nasir NAAM, Ishak, A, Pop I and Zainuddin N. MHD stagnation point flow towards a quadratically stretching/shrinking surface, *Journal of Physics: Conference Series* 1366 (2019), 012013. https://doi.org/10.1088/1742-6596/1366/1/012013